JOURNAL OF MATERIALS SCIENCE 26 (1991) 6119–6126

Electrochemical method for the investigation of transport properties of alumina scales formed by oxidation

Part II *Scale formed on a β-NiAl alloy*

D. NICOLAS-CHAUBET, A. M. HUNTZ, F. MILLOT
Institut de Science des Matériaux, Université Paris XI, 91405 Orsay, France

An electrochemical method based on plotting the *V–I* curves of an oxide scale was used to study the variation of transport properties across the α-alumina scale formed on β-NiAl at 1100 °C after 4 days of oxidation. The theoretical approach of *V–I* curves has been developed in part I. Analysis and comparison of the *V–I* curves obtained for different P_{O_2} imposed on alumina allowed us to propose a variation of ionic and electronic conductivities versus P_{O_2} inside the scale. Electronic and ionic conductivity variations so obtained are discussed. A volume conduction model of nickel-doped alumina is proposed for electronic conductivity. Diffusion of charged species along grain boundaries of α-alumina is suggested to be the main contribution to the ionic conductivity, and also to the transport during β-NiAl oxidation at 1100 °C.

1. Introduction

The aim of this work is to determine the transport properties of alumina scales, formed by oxidation of a β-NiAl alloy at 1100 °C. The study is carried out at high temperature, under oxidation conditions, with an electrochemical method based on plotting the current—potential curves of the corrosion scales. A preliminary theoretical study has shown that the analysis and comparison of such curves, obtained for various oxygen partial pressures imposed on the outer surface of the alumina scale, allow one to propose diagrams for the variation of the conductivity versus oxygen partial pressure inside the oxide [1].

2. Experimental procedure

2.1. Material

A β-NiAl, with 50.10 at % Ni was used. It was prepared by arc-melting under argon at CEN Saclay. The ingot was then annealed for 3 days in purified argon. The chemical composition of the alloy is reported in Table I.

The sample (20 mm × 9 mm × 2 mm) is mechanically polished on SiC paper up to 1200 grade on every face. It is then polished with alumina up to 0.5 μm particle size on only one large face (the one on which electrodes will be put).

2.2. Experimental device

In order to plot the characteristic curves, the electrical circuit schematized in Fig. 1 is set up. A stabilized current source can provide variable current from 0 to 32 mA. A voltmeter V (Model 6266, Enertec Schlumberger, Vélizy, France), with 0.2 μV accuracy and $10^{12}\,\Omega$ input impedance, is connected to a computer (Enertec 7066, Enertec Schlumberger). The current I in the external circuit is deduced from the potential difference V_1 measured by a voltmeter, in parallel connection with a resistance R_1 (100 Ω) in series with the oxide scale.

The experimental device was designed and described earlier by Ben Abderrazik *et al.* [2]. It is connected to a closed gas circuit, schematized in Fig. 2. A membrane pump allows gas circulation. Oxygen partial pressures varying from 10^5 to 10^{-5} Pa are obtained by Ar–O_2 and Ar–CO_2 mixtures. Oxygen partial pressures are measured by a zirconia gauge, with the oxygen partial pressure of Ni–NiO equilibrium (P_{O_2} (ref) = $10^{-3.9}$ Pa at 1100 °C). Samples are oxidized at 1100 °C for 4 days in pure oxygen before electrical measurements are undertaken. A previous study of the oxidation kinetics has shown that the growth of the scale after 4 days of oxidation is slow enough to be neglected during the electrochemical measurements [3–5].

2.3. Characterization of oxide scale

During the earlier study of the oxidation of β-NiAl at 1100 °C in O_2, the alumina scales formed were characterized [3–5]. The scale, about 3 μm thick after 4 days

TABLE I Chemical composition of β-NiAl alloy

Ni	Al	C	Co	Fe	Cu
68.6 wt %	31.4 wt %	28 ± 5 p.p.m.	<100 p.p.m.	34 p.p.m.	27 p.p.m.

0022–2461/91 $03.00 + .12

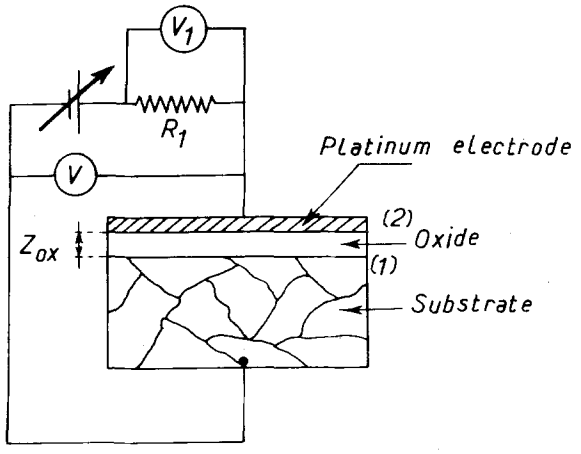

Figure 1 Equivalent electrical circuit used to plot the characteristic *V–I* curves.

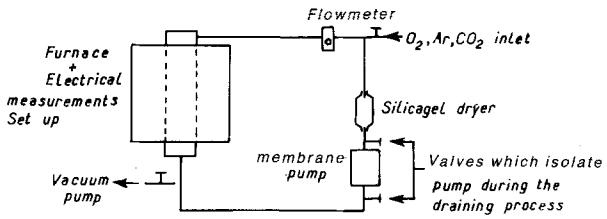

Figure 2 Gas circuit.

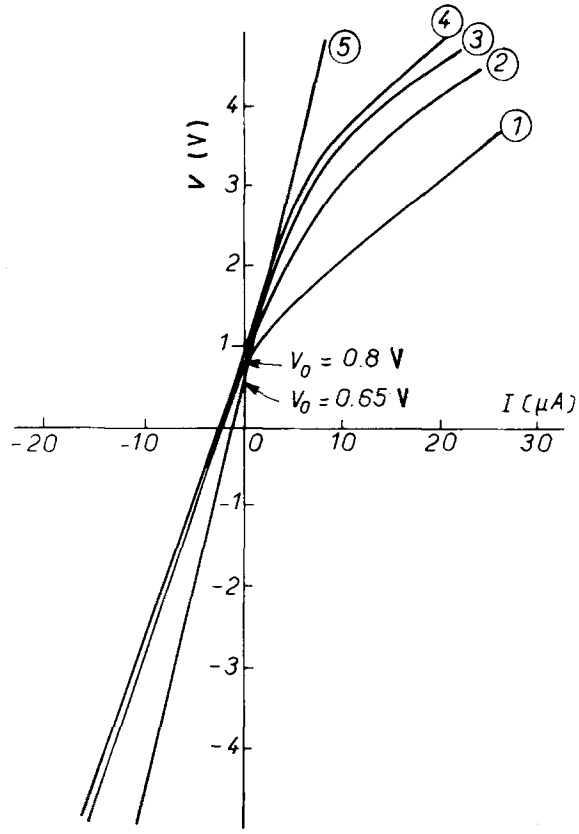

Figure 3 Evolution of the *V–I* curves with P_{O_2} for alumina scales formed at 1100 °C on β-NiAl. P_{O_2} (Pa) = (1) $10^{2.7}$, (2) $10^{-0.8}$, (3) $10^{-2.1}$, (4) 10^{-3}, (5) 10^{-5}.

of oxidation, is constituted by nickel-doped α-alumina probably in equilibrium with nickel-rich precipitates: X-ray photoelectron spectroscopy (XPS) showed that nickel was present near the outer surface of the scale in a small concentration, lower than 1 at % (thickness explored = 20 nm). The chemical state of nickel, which did not seem to be oxidized, could not be determined. Secondary ion mass spectroscopy (SIMS) analyses were undertaken as far as 100 nm depth and nickel-rich precipitates were found.

3. Determination of transport properties of alumina scale

3.1. Conductivity variations

Characteristic current–potential curves were determined for oxygen partial pressures, P_{O_2}, varying from 10^5 to 10^{-5} Pa. The curves so obtained are plotted in Fig. 3.

Evolution of the *V–I* curves will be now discussed. First, consider the *V–I* curve corresponding to 10^5 Pa: it is not a straight line, thus indicating that the conductivity varies along the oxygen chemical potential gradient of the scale. Comparison of the slopes of the "ionic" and "electronic" branches (see part [1]) indicates that the electronic conductivities are greater than the ionic conductivity values. Moreover, the linearity of the ionic branch suggests that there exists a P_{O_2} domain where $t_i \simeq 1$ and σ_i varies slightly ($t_i = \sigma_i/\sigma$ where σ_i is the ionic conductivity and σ the total conductivity).

No more information can be deduced from a single curve. In particular, it is impossible to determine whether the ionic conductivity corresponds to high or low oxygen chemical potentials. In order to resolve this question, it is necessary to examine the evolution of *V–I* curve shapes for different P_{O_2} [1].

From the variation of the slopes at characteristic points of the *V–I* curves when P_{O_2} decreases from 10^5 to 10^{-3} Pa, the following assertions can be suggested:

(i) As only the electronic branch is modified by the P_{O_2} decrease, it can be deduced that electronic conduction dominates for the highest oxygen chemical potentials existing in the scale.

(ii) V_0, the electrical potential difference between the inner and the outer interfaces, slightly changes. V_0 is given by the generalized Nernst–Einstein relation

$$V_0 = \int_1^2 \frac{t_i}{4F} d\mu \qquad (1)$$

For oxygen chemical potentials associated with P_{O_2} varying from 10^5 to 10^{-3} Pa, $t_i \simeq 0$.

(iii) In addition, the slope of the electronic asymptotic branch varies only slightly so $\sigma[\mathrm{Min}(\sigma_i/\sigma_e)] \sim$ const. for $10^{-3} < P_{O_2} < 10^5$ Pa.

(iv) The ionic branch remains linear: this means that ionic conductivity dominates for low oxygen potential and is probably constant in this range of P_{O_2}.

Another *V–I* curve has been determined for $P_{O_2} \simeq 10^{-5}$ Pa. A linear variation of V with I is observed: this means that the same conductivity type is predominant in the range of P_{O_2} between 10^{-5} Pa and the inner interface P_{O_2} value.

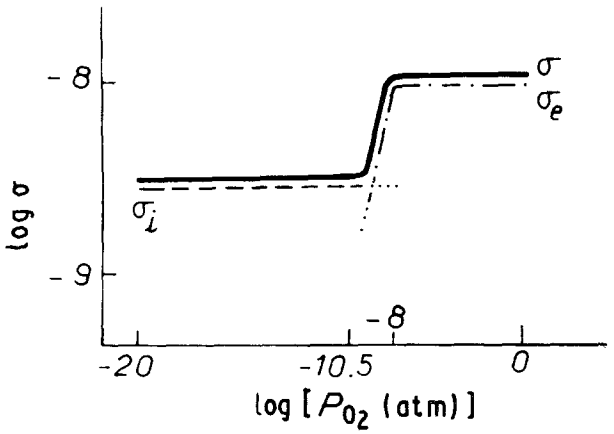

Figure 4 Variation of the conductivity with P_{O_2} inside the alumina scale.

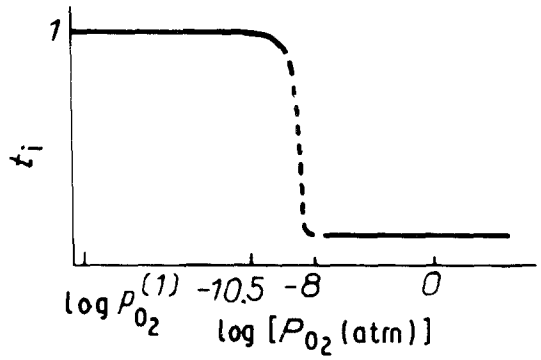

Figure 5 Variation of t_i with P_{O_2} inside the alumina scale.

V_0 now has a lower value than that determined for $10^{-3} < P_{O_2} < 10^{5}$ Pa. According to Equation 1, this indicates that t_i has increased from its previous value and that the predominant conductivity is ionic. From these two results, it is possible to conclude that $t_i \simeq 1$ for an oxygen chemical potential such that $10^{-3} < P_{O_2} < 10^{-5}$ Pa. Figs 4 and 5 summarize the results obtained from the analysis of the evolution of the V–I curves with decreasing P_{O_2}.

3.2. Determination of oxygen partial pressure at the β-NiAl–Al_2O_3 interface

According to the fact that, for $P_{O_2} \lesssim 10^{-5}$ Pa, t_i keeps a constant value about equal to unity, it is possible to determine the oxygen partial pressure at the NiAl–Al_2O_3 interface, $P^{(1)}_{O_2}$, from the generalized Nernst–Einstein Equation 1 and taking $V_0 = 0.65$ V, i.e. the value determined when $P^{(2)}_{O_2} = 10^{-5}$ Pa (see Fig. 3), $P^{(2)}_{O_2}$ being the outer oxygen pressure imposed on the scale. Equation 1 may be written in this case

$$V_0 = \frac{RT}{4F} \ln\left(\frac{P^{(2)}_{O_2}}{P^{(1)}_{O_2}}\right) \qquad (2)$$

Two $P^{(1)}_{O_2}$ is calculated: $P^{(1)}_{O_2} = 10^{-15}$ Pa. This value is markedly greater than the value obtained from the aluminium activity values in NiAl determined by Steiner and Komarek [6], i.e. 10^{-25} Pa.

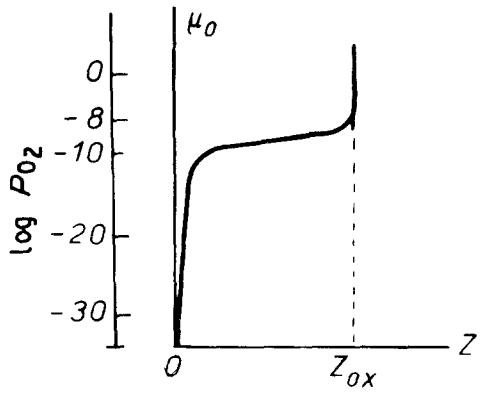

Figure 6 Scheme of the evolution of the oxygen chemical potential in the alumina scale.

3.3. Determination of oxygen chemical potential variation inside the scale

It is interesting and original to point out the variation of the oxygen chemical potential inside the scale. It must be remarked that this variation has never been determined and is, in most cases, approximated by a straight line joining the oxygen chemical potential extreme values.

Using the formalism established in part I of this paper [1], the expression for the oxygen chemical potential gradient, $\nabla\mu$, is given by [4, 5]

$$\nabla\mu = \frac{4F^2 J_i}{\sigma}\left(\frac{1}{t_i} + \frac{1}{1 - t_i}\right) \qquad (3)$$

According to this equation, it can be seen that $\nabla\mu$ depends both on σ and t_i. However, as σ varies only slightly in the $[\mu^{(1)}, \mu^{(2)}]$ domain, the evolution of $\nabla\mu$ can be qualitatively discussed by considering only t_i variations.

From Equation 3, it can be predicted that when $t_i = 0$ or $t_i = 1$, $\nabla\mu$ becomes very high. On the other hand, the minimum of $\nabla\mu$ is obtained for t_i close to 0.5. These remarks, when applied to our results, allow us to propose the diagram shown in Fig. 6 for the variation of μ versus the thickness of the scale Z_{ox}. The most important variations take place near the interfaces, over a very small thickness.

4. Discussion

4.1. Introduction

Numerous parameters may act upon the transport properties of thermally grown alumina (i.e. that developed by oxidation). Among them, the impurity content has a strong influence, considering the extrinsic conduction properties of alumina, and the relatively low experimental temperature (1100 °C). As nickel was found in the scale at about 1%, nickel doping must be discussed. Another parameter that must be considered is the oxygen partial pressure, as an important chemical potential gradient exists in the scale.

In the particular case of corrosion scales, other parameters may also act: the alumina microstructure

(the grain size in alumina scales is of the order of 1 μm), or the stresses in the scale. It has been suggested that stresses inside the scale may result in an increase of oxygen partial pressure at the inner interface [7]. The influence of grain boundaries on conductivity is not well known at this date. Kitazawa and Cobble [8] and Norby and Kofstad [9] suggested that grain boundaries enhanced the electronic conductivity of synthetic alumina. However, Petot-Ervas *et al.* [10] showed that the electrical conductivity of synthetic yttrium-doped alumina slightly depended on grain boundaries, in contradiction with the previous authors.

4.2. Nickel doping effect in alumina scale

As nickel is the major impurity in the scale, the possibility of the conduction properties of the scale being determined by the volume defects of nickel-doped alumina was considered.

4.2.1. Variation of nickel concentration inside the scale

The conduction properties of the alumina scale depend on the dissolved nickel content in grains, which varies with the oxygen chemical potential gradient existing in the scale. It was therefore interesting to know more about the nickel content variation inside the scale. Unfortunately it was not possible to measure such a variation. Nickel was only analysed close to the outer surface, and about 1 at % was found at about 20 nm depth. A theoretical approach based on thermodynamic considerations was therefore made in order to determine the variation of nickel solubility limit in the oxygen partial pressure gradient in the scale. This approach is detailed in the Appendix. The main conclusions can be summarized as follows (see Fig. 7):

(i) In the domain of the highest oxygen pressures in the scale ($P_{O_2} > 10^{-5}$ Pa) the nickel limit of solubility strongly increases as P_{O_2} decreases.

(ii) For intermediate P_{O_2} values ($10^{-21} \leqslant P_{O_2} \leqslant 10^{-5}$ Pa), the nickel solubility limit approximately keeps a constant value.

(iii) For lower oxygen pressures, the nickel solubility limit then decreases first slightly, and then curves more appreciably.

It has been shown that the highest variations of μ_{O_2} take place near the interfaces over a very small thickness. Variation of the nickel solubility limit can thus be schematized as in Fig. 8. In order to plot this curve with an order of magnitude for the values of the nickel solubility limit, a value equal to 7 p.p.m. was taken at 1100 °C in $P_{O_2} = 10^5$ Pa according to the results of Ando *et al.* [11].

Considering the plot of μ_{Ni} in Fig. 7, it can be noted that a nickel solubility of about 1% is not excluded for

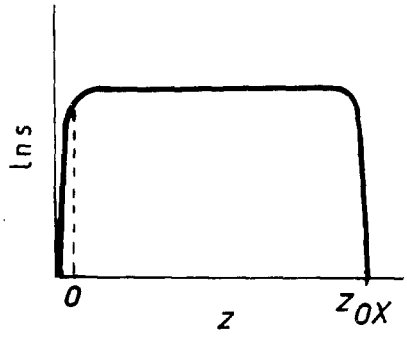

Figure 8 Shape of the nickel solubility variation versus the thickness Z of the alumina scale. $P_{O_2}^{(1)} = 10^{-15}$ Pa.

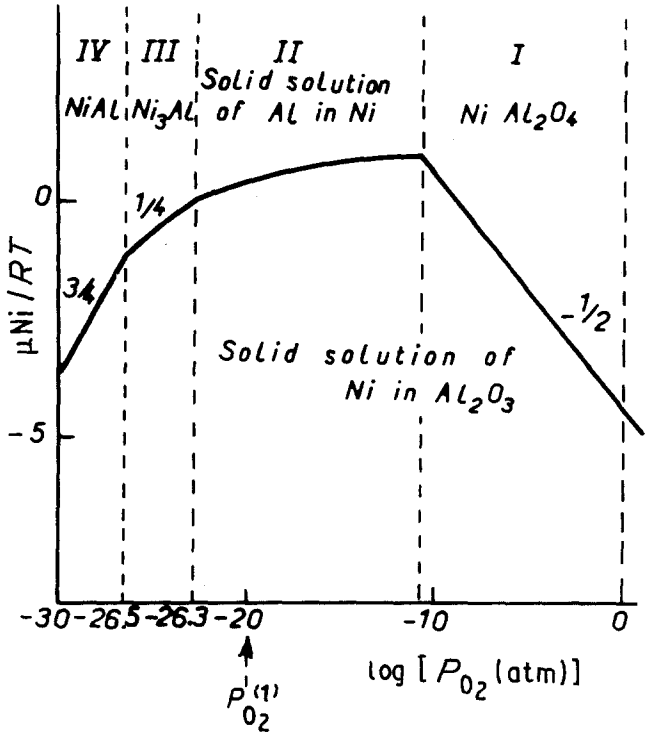

Figure 7 Prediction of the μ_{Ni} variation versus P_{O_2} in the scale from thermodynamic considerations. The nature of a possible secondary phase is indicated. $\mu_{Ni} \simeq 0$ was chosen for Ni–NiO equilibrium.

$P_{O_2} \sim 10^{-10}$ atm. This suggests that such a concentration ($\sim 1\%$) can be representative of the dissolved nickel in most of the thickness of the oxide scale (see Fig. 6). This order of magnitude corresponds to the results obtained by XPS for the nickel concentration, at least for small depths in the scale ~ 20 nm from the outer surface. At slightly greater depth, ~ 100 nm from the outer surface, small precipitates enriched in Ni were detected by SIMS.

So it can be suggested, from all these theoretical and experimental considerations, that in most of the thickness of the scale, about 1% Ni is in solid solution in Al_2O_3, coexisting with some Ni-enriched precipitates.

4.2.2. Model conduction by the volume of nickel-doped alumina

A model of conduction by defects in the volume of alumina grains can be proposed. It is based on Chen and Kröger's results on the conductivity of synthetic monocrystalline nickel-doped alumina [12].

According to their work, the dissolved nickel can exist with two possible states in alumina: Ni^{2+} ions for low oxygen chemical potentials, and Ni^{3+} ions for high oxygen chemical potentials. Possible defect equilibria are given by Equations 4 and 5 (Vink and Kröger's notation):

$$\tfrac{1}{2} O_{2g} + V_O^{2\cdot} + Ni'_{Al} = O_O^X + 2Ni_{Al}^X \quad (4)$$

$$Ni_{Al}^X = Ni'_{Al} + h \quad (5)$$

K_1, K_2 being the equilibrium constant for Equations 4 and 5, respectively, it can be shown that

$$[h^{\cdot}] = 2^{-1/3} K_2 K_1^{-1/3} [Ni_{Al}^X]^{1/3} P_{O_2}^{1/6} \quad (6)$$

Electronic conductivity being ensured by positive holes, it is proportional to

$$[Ni_{Al}^X]^{1/3} P_{O_2}^{1/6}:$$

$$\sigma_e \propto [Ni_{Al}^X]^{1/3} P_{O_2}^{1/6} \quad (7)$$

Chen and Kröger showed that, for monocrystalline nickel-doped alumina, all nickel in solution is Ni^{3+}, at 1500 °C for high oxygen partial pressures. If it is assumed that this is still true for the alumina scales at 1100 °C, $[Ni_{Al}^X]$ is proportional to the nickel concentration in the alumina grains. Then

$$\sigma_e \propto s^{1/3} P_{O_2}^{1/6} \quad (8)$$

In the Appendix, it appears that in the domain of the highest pressures in the scale, the limit of solubility of nickel varies as $P_{O_2}^{-1/2}$. σ_e is therefore expected to be invariant with P_{O_2} in this domain of "high pressures". As P_{O_2} decreases, one of the two following conditions is no longer true:

(i) Ni^{3+} is the dominating chemical state of dissolved nickel;

(ii) The concentration of dissolved nickel, i.e. the nickel limit of solubility, varies as $P_{O_2}^{1/2}$.

The electronic conductivity is then expected to decrease. It can be seen in Fig. 4 that the electronic conductivity variation is in agreement with the behaviour predicted by the defect volume conduction model.

An attempt was made to compare the order of magnitude of the electronic conductivity, estimated from *V–I* curves, with the order of magnitude of electronic conductivity for acceptor-doped alumina from the literature [8, 12, 13]. As studies for temperatures as low as 1100 °C are not numerous [8], results obtained for higher temperature ($T > 1300$ °C) were extrapolated. The values obtained are between 10^{-8} and $10^{-5.5}\ \Omega^{-1}\ cm^{-1}$, i.e. higher or equal to the order of magnitude of the higher electronic conductivities estimated from *V–I* curves ($10^{-8}\ \Omega^{-1}\ cm^{-1}$). So it can be remarked that an increase of electronic conductivity by grain boundaries is not obvious.

From Kroger's work the ionic conductivity is ensured by oxygen vacancies, $V_O^{\cdot\cdot}$, which are the main defects balancing Ni'_{Al}: σ_i is proportional to $[V_O^{\cdot\cdot}]$ and so to $[Ni'_{Al}]$. Thus, for the lowest pressures, as Ni^{2+} is the dominating chemical state for dissolved nickel, ionic conductivity should vary with P_{O_2} like the nickel concentration, i.e. σ_i would increase as P_{O_2} increases. For higher P_{O_2}, as Ni^{2+} is no longer the major state for dissolved nickel, a strong decrease of σ_i is expected as P_{O_2} increases. These predictions of the volume conduction model are in disagreement with the invariance of σ_i determined from *V–I* curves (Fig. 4). A model of volume conduction does not seem satisfactory to account for ionic conduction.

A comparison with the values of ionic conductivity for acceptor-doped alumina from the literature was done, with extrapolation at 1100 °C as previously. The order of magnitude obtained was $5 \times 10^{-11}\ \Omega^{-1}\ cm^{-1}$ [12, 13]. The order of magnitude of σ_i in the alumina scales formed on β-NiAl was estimated to be 100 times higher, about $3.5 \times 10^{-9}\ \Omega^{-1}\ cm^{-1}$.

4.3. Transport in alumina scale during oxidation

It was interesting to know the respective contributions of charged and neutral species to the transport during oxidation. By electrochemical measurements, the variations of the whole conductivity σ, and of the ionic transport number t_i, with the oxygen chemical potential were determined. These parameters can allow one to calculate a parabolic constant of oxidation, k_c, according to the formula

$$k_c = \frac{V}{12F^2} \int_{\mu^{(1)}}^{\mu^{(2)}} t_i(1 - t_i)\sigma \, d\mu \quad (9)$$

with V the molar volume of alumina and F the Faraday number; $\mu^{(2)}$ and $\mu^{(1)}$ are the oxygen chemical potentials at the outer and inner interfaces of the scale, respectively.

The calculated k_c value will be representative of an alumina growth due only to the diffusion of charged species, whereas the experimental k_c values determined during the β-NiAl oxidation study [3–5] are representative of the diffusion of all species, charged and neutral.

Using the formula above, and with some approximations, it was found that $k_c \simeq 2 \times 10^{-14}\ cm^2\ s^{-1}$.

The experimental value of the parabolic constant determined during the oxidation kinetic study at 1100 °C was $(k_c)_{exp} \simeq 2.8 \times 10^{-13}$ cm^2 s^{-1}. Considering that k_c is a sub-estimated value (because of approximations), it can be considered that k_c and $(k_c)_{exp}$ are of the same order of magnitude. From this comparison it can be concluded that the growth of the alumina scale on β-NiAl occurs mainly by the diffusion of charged species.

Moreover, in the oxidation kinetic study, a comparison of $(k_c)_{exp}$ and the diffusion coefficients for oxygen in alumina has shown that the diffusion paths during oxidation were grain boundaries [3–5]. Thus the growth of the scale mainly results from charged species diffusion in grain boundaries. This is in opposition with Kröger's assumption of grain boundary diffusion in alumina being controlled by neutral species transport [14, 15].

It can further be suggested that ionic conductivity is mainly intergranular. This could account for the high values obtained for ionic conductivity in the alumina corrosion scales.

5. Conclusions

An electrochemical method was used in order to study the transport properties of alumina scale resulting from β-NiAl oxidation at 1100 °C in oxygen. It has been shown that this method allows a relatively accurate, even if semi-quantitative, description of the transport properties of the scale.

From the variation of *V–I* curves determined for different oxygen partial pressures imposed on the oxide, it has been possible to propose a diagram of the variation of ionic and electronic conductivities inside the corrosion scale. Furthermore, in the particular case of the alumina formed on β-NiAl, the oxygen chemical potential variation in the thickness of the scale could be estimated. It was observed that the oxygen chemical potential slightly varies in the major part of the scale. The strongest variations of μ_{O_2} take place near the inner and outer interfaces.

Electrical properties of the scale have been discussed. An extrinsic nickel-doping effect can explain the electronic conduction properties of the alumina scale. On the other hand, this volume conduction model cannot account for ionic conductivity.

Ionic conductivity must be mainly intergranular and does not seem to depend on the oxygen partial pressure in the domain where σ_i is the major contribution to the total conductivity.

This work also indicated that transport during oxidation mainly results from charged species diffusion in alumina grain boundaries.

This study showed the interest of *V–I* curves as a method to determine transport properties. It could be interesting to use this method to investigate the influence of active elements, such as yttrium, on alumina transport properties, as this influence is still to be discussed.

Appendix: Estimation of the variation of nickel solubility with oxygen chemical potential in the alumina scale formed on β-NiAl

The evolution of the concentration of nickel dissolved in alumina, in the oxygen chemical potential gradient in the scale, is an important parameter determining the variation of conduction properties inside the scale. It has not been possible to experimentally determine this evolution. Thus, we tried to estimate it on the basis of thermodynamic considerations.

Let us consider that the concentration of nickel in the scale is higher than the limit of solubility of nickel. Then nickel in solution in alumina is assumed to be in equilibrium with the nickel precipitated phase. The nature of this phase may change as the oxygen chemical potential decreases in the scale. As μ_{O_2} decreases from the Al_2O_3–gas interface to the NiAl–Al_2O_3 interface, the phases in equilibrium with alumina are

NiO, $NiAl_2O_4$, $NiAl_x$ (solid solution of Al in Ni), Ni_3Al, NiAl

In fact, at 1100 °C, NiO reacts with alumina to form the spinel $NiAl_2O_4$ (because ΔG for this reaction is negative), provided that the oxygen flux across the scale is great enough.

The limit of the P_{O_2} domains for each phase has been calculated from the formation energy of the phase, ΔG, and the aluminium activities in the Ni–Al system determined by Steiner and Komarek [6]:

$NiAl_2O_4$:	$10^{-5.2}$	$\leqslant P_{O_2} \leqslant$	10^{5} Pa	Domain I
$NiAl_x (0 < x < 0.15)$	$10^{-21.3}$	$\leqslant P_{O_2} \leqslant$	$10^{-5.2}$ Pa	Domain II
Ni_3Al	$10^{-21.5}$	$\leqslant P_{O_2} \leqslant$	$10^{-21.3}$ Pa	Domain III
NiAl	$10^{-24.9}$	$\leqslant P_{O_2} \leqslant$	$10^{-21.5}$ Pa	Domain IV

For each domain, it is possible to write the Gibbs–Duhem relation:

$$S d\mu_{Ni} + 2 d\mu_{Al} + \tfrac{3}{2} d\mu_{O_2} = 0 \quad \text{in nickel-doped } Al_2O_3 \qquad (A1)$$

$$d\mu_{Ni} + 2 d\mu_{Al} + 2 d\mu_{O_2} = 0 \quad \text{in } NiAl_2O_4 \qquad (A2)$$

$$d\mu_{Ni} + x d\mu_{Al} = 0 \quad \text{in } NiAl_x \qquad (A3)$$

$$3 d\mu_{Ni} + d\mu_{Al} = 0 \quad \text{in } Ni_3Al \qquad (A4)$$

$$d\mu_{Ni} + d\mu_{Al} = 0 \quad \text{in NiAl} \qquad (A5)$$

where S is the atomic concentration of dissolved nickel in alumina.

Assuming that there is an equilibrium between the alumina solid solution and the precipitates, μ_{Al}, μ_{O_2} and μ_{Ni} are the same in the two phases. From Equations A1 to A5 successively, it is possible to express $d\mu_{Ni}/d\mu_{O_2}$ in each domain. The variation of μ_{Ni} in the scale can thus be determined. However, the interesting parameter is the solubility variation $ds/d\mu_{O_2}$. The relationship between μ_{Ni} and S is not obvious (except for low concentrations of dissolved nickel where $d\mu_{Ni} = RT \ln S$). However, the variations of μ_{Ni} and S are of the same order of magnitude, and variations of μ_{Ni} are certainly indicative of S variations.

The expressions for $d\mu_{Ni}/d\mu_{O_2}$ obtained in each domain are as follows. In domain I

$$\frac{d\mu_{Ni}}{d\mu_{O_2}} = -\frac{1}{2(1-S)} \qquad \text{(A6)}$$

Recent studies on the solubility of nickel in alumina have shown that it is very low at 1100 °C: 7 ppm. [11]. So, in domain I, we shall consider that S can be neglected in comparison with unity, so $d\mu_{Ni}/d\mu_{O_2} \simeq -1/2$. In this domain, the solubility increases as P_{O_2} decreases.

In domain II

$$\frac{d\mu_{Ni}}{d\mu_{O_2}} = \frac{3}{2}\frac{x}{(2-Sx)} \qquad \text{(A7)}$$

where x is the concentration of Al in Ni. We showed that for alumina formed at 1100 °C on β-NiAl, the oxygen chemical potential varies strongly and mainly near the inner and outer interfaces. So we assumed that the nickel concentration determined at 20 nm from the outer interface is already the concentration of dissolved nickel associated with oxygen chemical potentials of domain II. It was shown by XPS analysis that S was lower than 1 at %, so Equation A7 can be approximated by

$$\frac{d\mu_{Ni}}{d\mu_{O_2}} \simeq \frac{3x}{4} \qquad \text{(A8)}$$

For the lowest values of x, $d\mu_{Ni}/d\mu_{O_2} \simeq 0$, and it increases slowly to the limit of domain II (towards low P_{O_2}).

In domain III

$$\frac{d\mu_{Ni}}{d\mu_{O_2}} = \frac{3}{2(6-S)} \qquad \text{(A9)}$$

If we consider again that in our scales S is low and does not exceed 1 at %, it can be seen that the slope $d\mu_{Ni}/d\mu_{O_2}$ is close to 1/4.

In domain IV

$$\frac{d\mu_{Ni}}{d\mu_{O_2}} = \frac{3}{2}\frac{1}{(2-S)} \qquad \text{(A10)}$$

Neglecting S again, it can be seen that, in this domain, the slope $d\mu_{Ni}/d\mu_{O_2}$ increases more with μ_{O_2} (the slope is close to 3/4).

All these considerations are summarized in Fig. 7, where μ_{Ni}/RT variations are plotted versus P_{O_2}. The reference for the ordinates is 7 p.p.m. at $P_{O_2} = 1$ atm [11].

It must be remarked that the values of P_{O_2} sharing the different domains are only indicative. Their values were calculated with Steiner and Komarek's data which disagree with our P_{O_2} value at the inner interface: a P_{O_2} equal to 10^{-15} Pa was found with electrical measurements at the NiAl–Al_2O_3 interface, higher than the value that can be calculated from Steiner and Komarek's results (10^{-25} Pa).

In conclusion, this analysis predicts an important increase of the solubility of nickel in the P_{O_2} domain I. Later, the solubility decreases in the other domains, very slowly on domain II, and then more quickly.

So, considering the solubility of nickel in alumina in pure oxygen at 1100 °C (about 7 p.p.m.) [11] and the variations predicted on the basis of thermodynamical considerations, a nickel solubility such as 1 at % could be observed in alumina, for P_{O_2} close to 10^{-10} atm. This corresponds to the observed nickel concentration in the scale.

For the chemical state of nickel in the scale, it implies that for the highest pressures, P_{O_2} close to 1 atm, nickel is both in solution and precipitated in alumina. For lower pressures, as the solubility increases, it can happen that nickel is only in solution in alumina, and not precipitated.

It has been shown that μ_{O_2} varies slightly in most of the thickness of the scale. So, considering the previous discussion of the evolution of the nickel solubility versus P_{O_2}, it can be thought that the nickel solubility varies slightly inside the scale, and that the average solubility is about the maximum value of Fig. 7.

References

1. D. NICOLAS-CHAUBET, A. M. HUNTZ and F. MILLOT, *J. Mater. Sci.* **26** (1991) in press.
2. G. BEN ABDERRAZIK, F. MILLOT, G. MOULIN and A. M. HUNTZ, *J. Amer. Ceram. Soc.* **68** (1985) 302.
3. D. NICOLAS-CHAUBET, C. HAUT, C. PICARD, F. MILLOT and A. M. HUNTZ, in Proceedings of 2nd International Symposium on High Temperature Corrosion, Les Embiez, France, May 1989, *Mater. Sci. Eng.* **A120** (1989) 83.
4. D. NICOLAS-CHAUBET, thesis, University of Paris XI, Orsay (1989).
5. *Idem., Métaux Corrosion et Industrie* No. 763 (1989) 61; 765–766 (1989) 121; 768 (1989) 191.
6. A. STEINER, K. L. KOMAREK, "Thermodynamic activities of Solid Nickel-Aluminum Alloys", Trans. AIME, 230 (1964) 786.
7. A. T. FROMHOLD, in Proceedings of Conference on "Stress Effects on the Oxidation of Metals", edited by J. V. Cathcart (Met. Soc. AIME, 1979) pp. 2–74.
8. K. KITAZAWA and R. L. COBLE, *J. Amer. Ceram. Soc.* **57** (1974) 245.
9. T. NORBY and P. KOFSTAD, in Proceeding of 5th International Conference on High Temperatures and Energy, High Temperatures, High Pressures, Rome, Italy, May 1987.
10. G. PETOT-ERVAS, D. DEWEIRDER, M. LOUDJANI, B. LESAGE and A. M. HUNTZ, "Nonstoichiometric compounds", in Advances in Ceramics, Vol. 25, edited by the American Ceramic Society (1987) pp. 123–135.

11. K. ANDO, M. MOMODA, T. AZUMI and S. KITAJAMA, *J. Amer. Ceram. Soc.* **70** (1987) C309.
12. J. S. CHEN and F. A. KRÖGER, *J. Mater. Sci.* **20** (1985) 3191.
13. C. R. KORIPELLA and F. A. KRÖGER, *J. Phys. Chem. Soc.* **47** (1986) 55.
14. L. D. HOU, S. K. TIKU, H. A. WANG and F. A. KRÖGER, *J. Mater. Sci.* **14** (1979) 1877.
15. F. A. KRÖGER, in "Advances in Ceramics", Vol. 10, edited by W. D. Kingery (American Ceramic Society Columbus, Ohio, 1984) p. 100.

Received 23 July 1990
and accepted 6 February 1991